The pathway from the solution to the steps

Peter G. Vekilov,[1,2,*] Lakshmanji Verma,[1] Jeremy C. Palmer,[1] Rajshree Chakrabarti,[1] and Monika Warzecha[3]

[1] *William A. Brookshire Department of Chemical and Biomolecular Engineering, University of Houston, 4726 Calhoun Rd., Houston, TX 77204-4004, USA.*

[2]*Department of Chemistry, University of Houston, 3585 Cullen Blvd., Houston, TX 77204-5003, USA*

[3]*EPSRC CMAC Future Manufacturing Research Hub, c/o Strathclyde Institute of Pharmacy and Biomedical Sciences, Technology and Innovation Centre, 99 George Street, Glasgow, G1 1RD, U.K.*

* *Correspondence and request for material should be addressed to P.G.V. (vekilov@uh.edu).*

Abstract

The pathway of solute access to the kinks is an issue of unparalleled fundamental significance that also carries severe consequences for the morphologies, quality, and, utility of the grown crystals. Here we review experimental tests to distinguish between the two pathways of solute supply to the steps: directly from the solution or after first adsorbing on the terraces between steps and diffusing along the crystal surface towards the steps. Generalizing the evidence accumulated with ionic, organic, protein, and biomineral crystals to-date, we put forth a criterion to predict the pathway of solute supply to the kinks. The proposed criterion relies on the interactions of the solvent with solute and the crystal surface. Solvents that strongly associate to the crystal surfaces and solute molecules weaken solute adsorption and contribute to faster surface diffusion and abundant solute supply to the steps, which, in turn, makes the surface diffusion pathway faster than the one directly from the solution. Solvents that do not attenuate

the solute-crystal surface attraction promote strong adsorption, which suppresses surface diffusion and encourages direct incorporation into the kinks. We propose that computational methods to predict *a priori* the pathway from the solution to the surface as a part of efforts to model crystal growth rates, morphologies, and quality need to faithfully account for solvent association to the crystal surfaces and to solute molecules.

Keywords

A1. solution growth

B1. mechanisms

A1. surface diffusion

B1. direct incorporation

A1. organic solvent

B1. aqueous solution

Introduction

In 1999 Alex Chernov gave the opening lecture at the Gordon Conference on Thin Film and Crystal Growth Mechanisms. In the subsequent discussion Alex stated that if he were allowed to ask God one question, it would be whether surface diffusion was possible in solution growth. Alex highlighted an issue of paramount fundamental significance, namely how solute molecules reach the steps before they incorporate in the crystal. Two pathways had been envisioned: directly from the solution (Fig. 1a) [1, 2] or after first adsorbing on the terraces between steps and diffusing along the crystal surface towards the steps (Fig. 1b) [3, 4]. The selection of a molecular pathway to the steps also has huge practical consequences. Attempts to predict *a priori* the growth rates of anisotropic crystal faces and, in this way, to evaluate the expected sizes and morphologies of crystals grown for numerous applications [5-7] rely on assumptions about how the molecules arrive at the steps. Furthermore, solute supply to a step from the crystal surface is constrained to two dimensions and more sensitive to the nearby presence of other steps that also consume solute. The competition for supply between closely-spaced steps introduces a positive feedback loop, whereby the closer the steps are, the more limited is the accessible solute, which pulls the steps even closer. The positive feedback and the resulting step-step attraction are substantially weaker if the steps feed directly from the solution [2, 8-10]. This strong attraction between the steps supplied from the surface destabilizes trains of equidistant steps at two lengthscales [11].

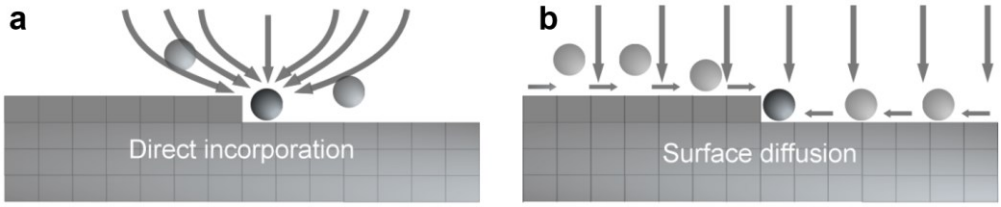

Fig. 1. Schematics of two pathways from solution to steps: direct incorporation, in **a**, and *via* adsorption on the terraces followed by diffusion towards the steps in **b**. Arrows indicate supply fluxes of solute, depicted as spheres, towards the steps.

At the lengthscale of the crystal face, step-step interaction *via* their surface supply fields enforces exaggerated response to the non-uniformity of supersaturation along the facet. Owing to

the spherical symmetry of the diffusion field, the edges of a polyhedral crystal are exposed to higher supersaturation than the facet centers (Fig. 2a). Alex Chernov was the first to point out that the preservation of the crystals shape in this non-uniform concentration field is due to an increase in the step density at the facet center; the step density increase coordinates with the slower step velocity to ensure uniform facet growth rate from the crystal edge to the facet center (Fig. 2a) [12, 13]. How close the steps can pull, however, is limited, for instance, by the extent of their intrinsic shape fluctuations, often called step width [11]. If the step density reaches its upper threshold, the face loses stability and a depression in its center evolves [14]. The attraction between steps that feed from the crystal surface enforces a multifold stronger response of the step density to the lower concentration at the facet center [15, 16]. The threshold step density is reached at much lower supersaturations, polyhedral crystal shapes are strongly destabilized, and the development of hollow (Fig. 2b), hopper-shaped (Fig. 2c), and dendritic (Fig. 2d) morphologies is promoted [17].

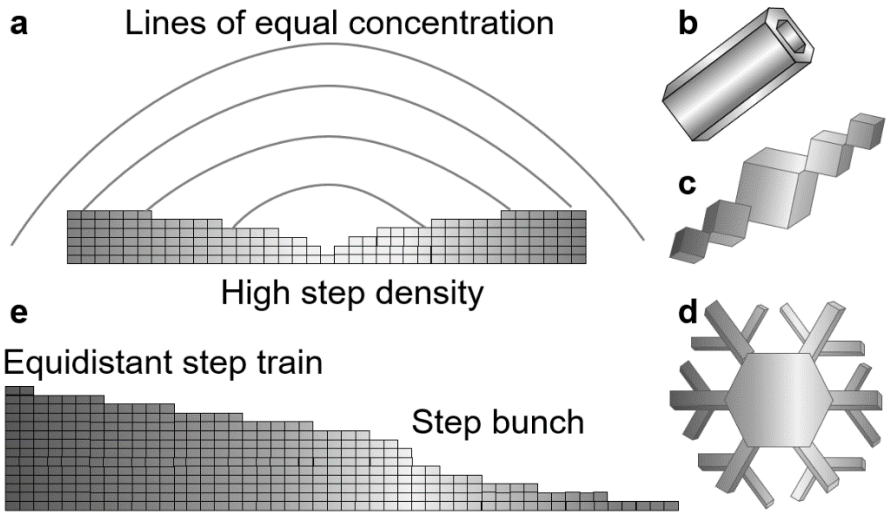

Fig. 2. Schematic illustrations of the effects of strong step-step interactions. **a.** Increasing step density due to lower concentration at the facet center that may trigger loss of crystal shape stability leading to hollow crystals, **b**, hopper growth, **c,** and dendrites. **d**. **e.** The formation of a step bunch due to step-step attraction.

At the lengthscale of step-step separation, the strong competition for supply between steps that grow by the surface diffusion mechanism induces step bunches (Fig. 2e) that may evolve into

macrosteps [18-20]. Step bunches and macrosteps may destroy the quality of the growing crystals. First, they may modify the incorporation of impurities and generation of vacancies in their wake and in this way striate the crystal [21, 22]. Second, macrosteps may fold to entrap microdroplets of solution and engender other three-dimensional crystal defects [8, 23]. The rationale contributed by Alex Chernov to understanding step bunching in solution growth [19, 24-33] was found to transfer to growth in high-vacuum environments and even to the effects of electric current on step patterns formation and evolution [34-36]. Employing the surface diffusion pathway to supply solute molecules to the steps contributes to much less stable step trains and substantially facilitates transitions to more varied crystal structures.

We scientists have the unique privilege to ask our respective deities questions. If we ask intelligently, they may answer. In the last 20 years, advanced methods have helped to accumulate substantial evidence to address the question posed by Alex Chernov in 1999. Here we review the tests that distinguish between the two pathways of solute supply to the steps and the systems for which one or the other pathway has been demonstrated. Generalizing the evidence accumulated so far, we formulate a criterion to predict the pathway of molecular access to the kinks.

The surface diffusion pathway

Sub-linear correlation between the step velocity and solute concentration

Crystal growth constitutes a bimolecular chemical reaction between kinks and solute molecules [37, 38]. Correspondingly, the rate of this reaction depends linearly on the concentrations of kinks and solute [1, 2]. Kinks locate along steps and the kink concentration is represented by kink density, i.e., the number of kinks per unit step length; if the step length is measured in number of molecules, the kink density is dimensionless and equal to the reciprocal average number of molecules between kinks. The kink geometry dictates that the kink density is limited from above [1, 39]. As such a limit, one can envision a step configuration with a kink density of 0.5, in which two molecules of a new row along the step alternate with two vacancies

(Fig. 3a). This configuration, however, is unique and would have zero entropy [40-42]. Careful evaluation indicates that maximizing the step entropy enforces more disordered configurations (Fig. 3b), for which the upper limit of kink density drops to ca. 0.3 [43]. If the bonds between molecules in the crystal lattice are relatively weak [1], this limit is reached even at equilibrium and the kink density does not depend on the supersaturation or undersaturation [44]. If the kink density is that high, constant, and independent of the solute concentration, the step velocity v, which is proportional to the rate of the reaction between kinks and solute, becomes proportional to the solute concentration C. Linear $v(C)$ correlations have been recorded for numerous solution-grown crystals [45-47].

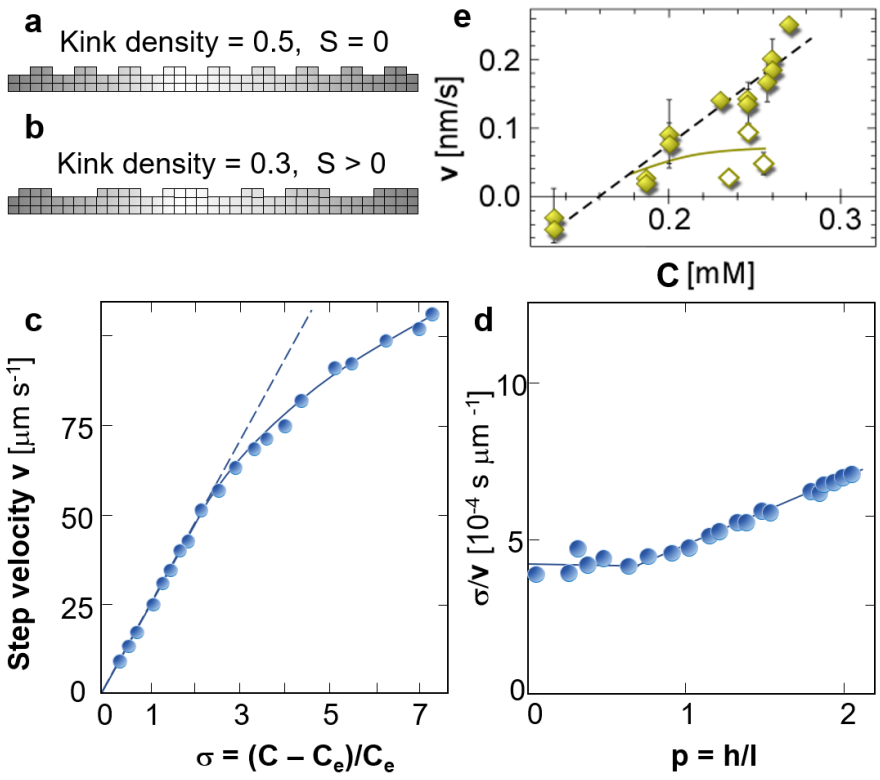

Fig. 3. Sublinear correlations of the step velocity *v* with the solute concentration *C*. **a, b.** Schematic representations of a highly ordered step edge configuration with the maximum possible kink density of 0.5 in **a**, and a disordered configuration with lower kink density but higher entropy *S* in **b. c, d.** Data for ammonium dihydrogen phosphate (ADP) crystals growing from an aqueous solution from [9, 10]. **c.** The $v(C)$ correlation; C_e is the solubility. **d.** The data in **c** in coordinates $[\sigma/v](p)$, where $\sigma = C\,C_e^{-1} - 1$ and $p = h/l$; h, step height, l, step separation. **e.** The $v(C)$ correlation for β-hematin crystals growing from a mixture of 95% volume % n-octanol and 5

volume % water from [48-50]. Solid symbols, for steps separated by l > 180 nm, v increases linearly with C [48]. Open symbols, for l < 180 nm, v is significantly reduced. Scatter in data for l < 180 nm is due to the strong dependence of v on l and the variation of l during the measurements.

If the kink density is lower than the thermodynamic limit of ca. 0.3—owing to, e.g., stronger intermolecular bonds in the crystal lattice—increasing solute concentration drives higher kink density [51] and superlinear increase of v with increasing supersaturation [30, 46, 47, 52, 53]. A superlinear $v(C)$ may also arise if a reaction between solute molecules produces a more growth-competent solute oligomer [54-56]. Importantly, none of these scenarios predicts a sublinear $v(C)$. Such a correlation would indicate the presence of additional resistance to solute incorporation into steps that only activates at high C. Sublinear $v(C)$ may represent an indication that solute is supplied to the steps *via* the crystal surface and the enhanced competition for supply between adjacent steps suppresses their response to increasing C.

A classical work [4] modeled the correlation between the step velocity v and the solute concentration C during crystal growth from solution. They assumed that the solute reached the steps *via* several sequential stages: diffusion through the solution to the crystal surface, adsorption to the terraces between steps, desorption back into the solution, two-dimensional diffusion along the surface towards the steps, and, finally, incorporation into steps. If transport of solute from the solution bulk toward the crystal surface is faster than the subsequent stages [9, 10, 57] the derived kinetic law transforms to

$$v = \frac{\lambda}{h}\frac{\Omega D}{\Lambda_{ads}}(C - C_e)\left(\frac{\Lambda_s}{\lambda} + \frac{1}{2}\coth\frac{l}{2\lambda}\right)^{-1}, \quad (1)$$

where h is step height, l is the separation between adjacent steps, λ is the characteristic length of surface diffusion, Ω is the molecular volume in the crystal, D is the bulk diffusivity, Λ_{ads} is a resistance to adsorb on the terraces from the solution in units of length, Λ_s is the resistance to incorporate into kinks from the surface, also measured as length.

The hyperbolic cotangent function is highly sensitive to small variations of its argument in the vicinity of unity. Accordingly, at $l = 2\lambda$ the correlation in Eq. (1) transitions between two

limiting cases. If $l > 2\lambda$, then $\coth(l/2\lambda) \cong 1$, and when $l < 2\lambda$, $\coth(l/2\lambda) \cong 2\lambda/l$. Denoting for brevity $(C - C_e)/C_e$ as σ, the scaling between v and C is linear for distant steps that do not compete for supply of solute, i.e, for which $l \gg 2\lambda$

$$\frac{\sigma}{v} = \frac{h\Lambda_{ads}}{\lambda\Omega C_e D}\left[\frac{\Lambda_s}{\lambda} + \frac{1}{2}\right], \quad (2)$$

and sublinear for closely spaced steps, for which $l \ll 2\lambda$ and decreases further at higher C

$$\frac{\sigma}{v} = \frac{h\Lambda_{ads}\Lambda_s}{\lambda^2\Omega C_e D} + \frac{\Lambda_{ads}}{\Omega C_e D}\frac{h}{l}, \quad . \quad (3)$$

The relations in Eqs. (2) and (3) predict sharp transition from a linear to a sublinear correlation between v and $(C - C_e)$ as l decreases with higher C (Fig. 3c, e) that is particularly conspicuous if the step velocity data are presented in coordinates $[\sigma/v](h/l)$ (Fig. 3d). In these coordinates, the proportionality between v and σ manifests as a constant value of σ/v for large step separations, corresponding to low h/l. The competition for supply between adjacent steps that arises at small l enforces a linear increase of σ/v with increasing h/l (Fig. 3d).

Closely-spaced steps also compete for supply from the solution bulk. Owing to the three-dimensional nature of diffusion in the solution, this competition is substantially weaker. An original model by Chernov [2, 8] predicted that in this case

$$v = \beta\Omega(C - C_e)\left[1 + \frac{\beta h\delta}{Dl}\right]^{-1}, \quad (4)$$

where β is the step kinetic coefficient and δ is the thickness of the concentration boundary layer controlled by the solution flow rate [2, 8, 58]. Using typical order-of-magnitude estimates for $\beta \approx 10^{-4}$ m s^{-1}, $h \approx 10^{-9}$ m, $\delta \approx 10^{-6}$ m, and $D \approx 10^{-9}$ m^2 s^{-1}, we obtain $v = \beta\,\Omega(C - C_e)\left[1 + \frac{10^{-10}\,\mathrm{m}}{l}\right]^{-1}$, i.e., the $v(C)$ correlation would deviate from linearity at l shorter than 1 nm, i.e., when two adjacent steps nearly merge into a double-height step. At the typical step separations of order 100 nm and more, the delay of step growth due to overlapping bulk supply fields is negligible [9, 10].

Based on the low sensitivity of the step velocity v to decreasing step separation l at high supersaturations for steps that directly feed from the solution, observed sublinear $v(C)$ correlations and sharp transitions between constant and linear $[\sigma/v](h/l)$ correlations have been interpreted as evidence that the solute reaches the steps via the crystal surface [9, 10, 48, 49, 57]. Notably, in all of these systems the solvents were fully or partially aqueous.

Closely spaced steps grow slower

The analytical expressions for the correlation between the step velocity v and the solute concentration C, Eqs. (1) – (3), suggest another criterion to discriminate between the two pathways for solute supply to the steps, the dependence of the step velocity v on step separation l. If the surface diffusion pathway is selected, closely spaced steps should grow slower. AFM observations with hematin [48-50, 59, 60], whose crystallization is a part of the heme detoxification mechanism of malaria parasites [61-63], reveal that the competition for nutrient supply between adjacent steps retards v, as observed for two steps separated by about 50 nm and growing towards each other (Figs. 4a–e) with $v \approx 0.05$ nm s^{-1}. Under identical conditions, steps

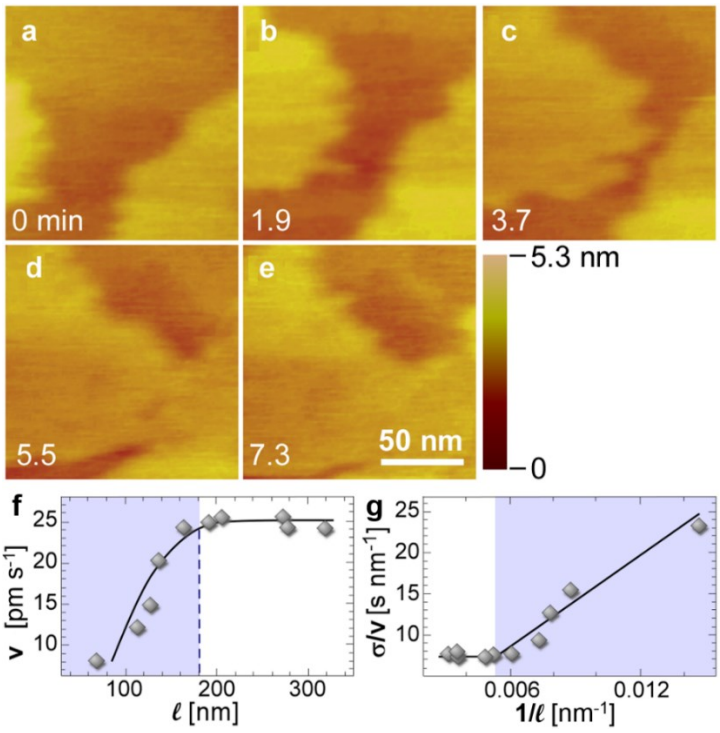

Fig. 4. Closely spaced steps grow slower. **a – e.** A sequence of *in situ* AFM images of a (100) face of a hematin crystal growing from a mixture of 95% volume % n-octanol and 5 volume % water at c_H = 0.23 mM, displaying the growth of two steps (left and right) in opposing directions. **f.** Step velocity v at c_H = 0.19 mM as a function of the interstep distance l. The step velocity v slows down at l < 180 nm, highlighted by shading. **g.** The data in f are replotted using coordinates $[\sigma/v](1/l)$. Shaded area corresponds to one in f.

separated by more than 180 nm move with v = 0.12 nm s^{-1} (Fig. 3c) [48, 49]. Additional observations of growing steps on hematin crystals revealed that groups of closely spaced steps move significantly slower than well separated steps (Fig. 4f). Again, in agreement with Eqs. (2) and (3) the ratio σ/v responds very sensitively to decreasing step separation l if plotted as a function of l^{-1} (Fig. 4g).

Slower motion of closely spaced steps compared to well separated steps has been recorded with numerous organic (olanzapine [54]), inorganic (ADP [9, 10]), biomineral (calcite [64]), and protein (lysozyme [15, 16, 65], canavalin [66], glucose isomerase [67], triosephosphate isomerase [68]) systems. The strong interaction between the steps has been viewed as evidence that the solute molecules reach the steps after two-dimensional diffusion along the surface [9, 10, 49, 57, 69].

Asymmetry of incorporation into the steps from the top and bottom terraces

If molecules first absorb on the terraces between steps and then diffuse towards the steps, they may incorporate into steps from both the upper and the lower terraces (Fig. 5a). The molecular configurations on approach to the step edge from the two adjacent terraces are distinct and suggest that the incorporation of molecules into steps from the upper and lower terraces may be asymmetric. Asymmetric incorporation has often been observed during step growth from the vapor via adsorption on the terraces and surface diffusion [70]; it is referred to as the Ehrlich-Schwoebel effect [71, 72]. Notably, such asymmetry is impossible if molecules arrive at the steps directly from the solution.

Pronounced asymmetry of molecular incorporation from the upper and lower terraces was observed for steps on a (100) β-hematin crystal surface (Fig. 5b) [48, 49]. To improve the time

resolution, these images were collected with disabled vertical scan axis so that the AFM tip continuously probed a single line parallel to the *c* crystallographic direction. The vertical axis in the collected AFM image represents time (Fig. 5b). The image presents the growth of two steps in the *c* direction. The height of each step is ~ 1.2 nm, consistent with the β-hematin crystal lattice parameter in the [100] direction [63]. In both the positive and negative *c* directions, the observed step pair is separated from other steps by about 200 nm, these steps are outside the imaged area.

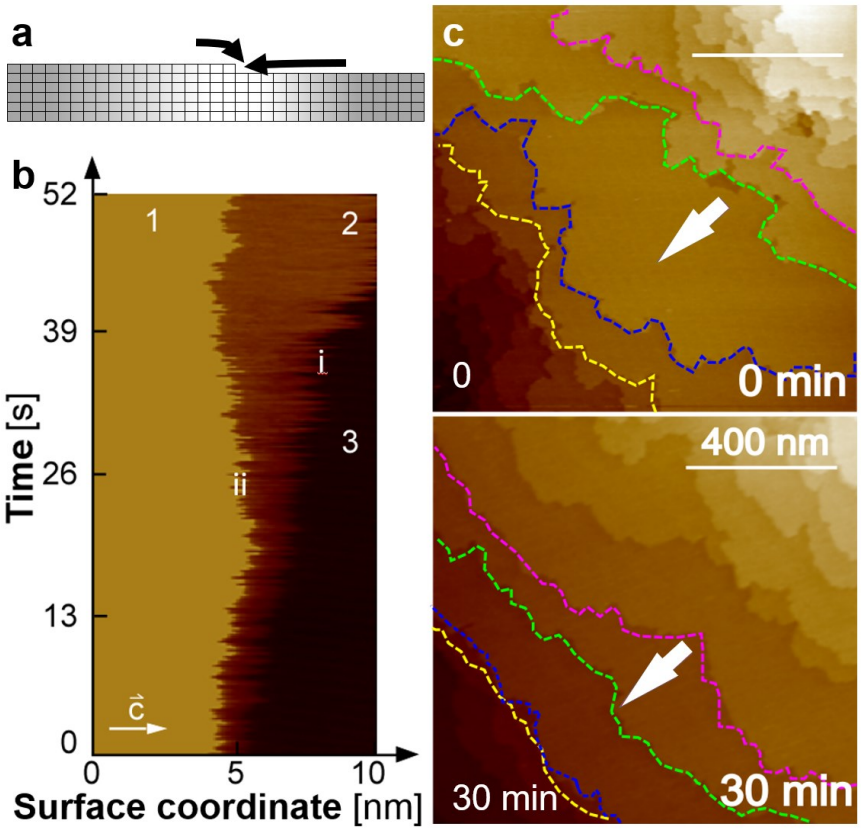

Fig. 5. Asymmetric incorporation into steps. **a.** Schematic of molecular fluxes into a step from the upper and lower terraces. **b.** *In situ* AFM image of two steps on a β-hematin crystal growing from a mixture of 95% volume % n-octanol and 5 volume % water at concentration *C* = 0.26 mM collected with a disabled vertical scan axis. In this imaging mode, the vertical axis represents time. *i* and *ii* denote a lower and higher step, respectively; 1, 2, and 3 label the terraces adjacent to these two steps. **c.** Evolution of the step configuration over 30 min during growth of olanzapine crystals from a 1:1 (vol) water/ethanol mixture at *C* = 2.38 mM. Thick white arrows indicate direction of step growth.

During 52 s of imaging the lower step, labeled as *i*, advances by about 5 nm, corresponding to $v \cong 0.1$ nm s^{-1} (Fig. 5a). During this time, the step velocity is relatively steady, with inevitable

fluctuations, despite the increasing separation from the higher step *ii*. The independence of the step velocity from the width of the higher terrace, labeled 2, indicates that its supply of solute from the side of terrace 2 is insignificant. Furthermore, the velocity of this step is in good agreement with the data collected with steps separated from their neighbors on both sides by more than 180 nm at the same C = 0.26 mM (Fig. 3e). This agreement suggests that step *i* receives a complete supply of molecules from the side of terrace 3, where a competing step is at a distance of about 200 nm. By contrast, step *ii* exhibits only fluctuations in its position and negligible net growth. Importantly, step *ii* does not grow even though it is separated from its competing step on terrace 1 by about 200 nm, suggesting that molecular incorporation from the side of the higher terrace is prohibitively slow.

Another example of asymmetric incorporation into steps was observed during the growth of crystals of olanzapine, an antipsychotic drug [73, 74], growing from a 1:1 water-ethanol mixture. Steps with broad front terraces and narrow rear terraces (such as the step highlighted in green in the central and right parts of Fig. 5c) grow faster than the step immediately behind them (e.g., the pink step), defined by a narrow front terrace and a broad rear terrace (Fig. 5c). In the left parts of the AFM images in Fig. 5c, the blue step escaping from the green step provides an analogous example. The accelerated step velocity in the presence of closely positioned (≤ 150 nm) rear steps suggests that the steps mostly feed from the front.

The observations of asymmetric incorporation into steps on both β-hematin and olanzapine crystal surfaces were supplemented by strong dependences of the step velocity on step-step separation to support the conclusion that, in both cases, the steps predominantly feed from the terraces between them [49, 50, 54].

The ratio of the incoming and outgoing fluxes into a kink

Even in a supersaturated solution, a substantial fraction of the solute molecules that have associated to a kink dissociate back to the crystal surface or into the solution [1, 2, 8]. The step

grows if the incoming flux overwhelms the outgoing flux and dissolves if, in an undersaturated solution, molecular retreat prevails. The law of mass action dictates that the incoming flux j_+, the number of molecules that incorporate into a kink per unit time, scales with the solute concentration C if the molecules reach the kinks directly from the solution, or with n_s, the surface concentration of adsorbed solute, if the steps feed from the surface. At equilibrium with the solution, $j_+ = j_-$, $C = C_e$, and $n_s = n_{se}$, where j_- is the outgoing flux, C_e, the solubility, and n_{se}, the equilibrium surface concentration. The outgoing flux j_- is independent of C or n_s and hence the net flux into a kink $(j_+ - j_-)$ scales with either $(C - C_e)$ or $(n_s - n_{se})$. Mass preservation dictates that the step velocity $v = \rho_k a(j_+ - j_-)$, where a is the molecular size, $\rho_k = 1/\bar{n}_k$ is the kink density, and $\bar{n}_k$ is the average number of molecules between kinks. These scaling relations are consistent with the kinetic laws for both the surface diffusion pathway, Eq. (1), and direct incorporation, Eq. (4).

The criterion for the solute incorporation pathway is based on the ratio j_+/j_-, which should equal C/C_e if the molecules reach the steps directly form the solution, or n_s/n_{se} for the surface diffusion pathway. At equilibrium, $C/C_e = n_s/n_{se} = 1$. In a supersaturated solution, however, n_s is constrained by the rates of adsorption and surface diffusion and lags behind C leading to n_s/n_{se} substantially lower than C/C_e. The surface concentrations n_s and n_{se} cannot be accurately evaluated. By contrast, both C and C_e are easily measured. Thus, the equality or inequality of the ratios j_+/j_- and C/C_e represent a powerful tool to discriminate between the two incorporation pathways [69].

AFM observations of the step edges during growth of crystals of the proteins ferritin, a mammalian iron storage protein [75-77], and apoferritin, in which the iron core has been removed, allowed evaluation of the upper bound of j_+/j_-. Pseudo-images, recorded with scanning disabled along the y-axis, so that the vertical coordinate becomes the time axis (Fig. 6), reveal both attachment and detachment events. For apoferritin, the net growth is three molecules (25

detected attachments and 22 detachments) for 165 s, leading to a net flux ($j+ - j-$) = 0.065 s^{-1} (Fig. 6a). For ferritin, growth over 128 s reveals 21 attachments events, 19 detachments, and an average net flux ($j+ - j-$) = 0.054 s^{-1} (Fig. 6b). For both crystals, the average kink density is ρ_k = 0.28 and the molecular size a = 13 nm [40-42, 69, 78-81]. The product $\rho_k a(j_+ - j_-)$ equals 0.25 nm s^{-1} for apoferritin and 0.20 nm s^{-1} for ferritin. Both values are very similar to independently measured step velocities at the respective supersaturations [40-42]. This correspondence indicates that the apoferritin and ferritin crystals grow by the attachment of single molecules to kinks located along the steps and validates the measurements of the net flux ($j_+ - j_-$) for the two crystals.

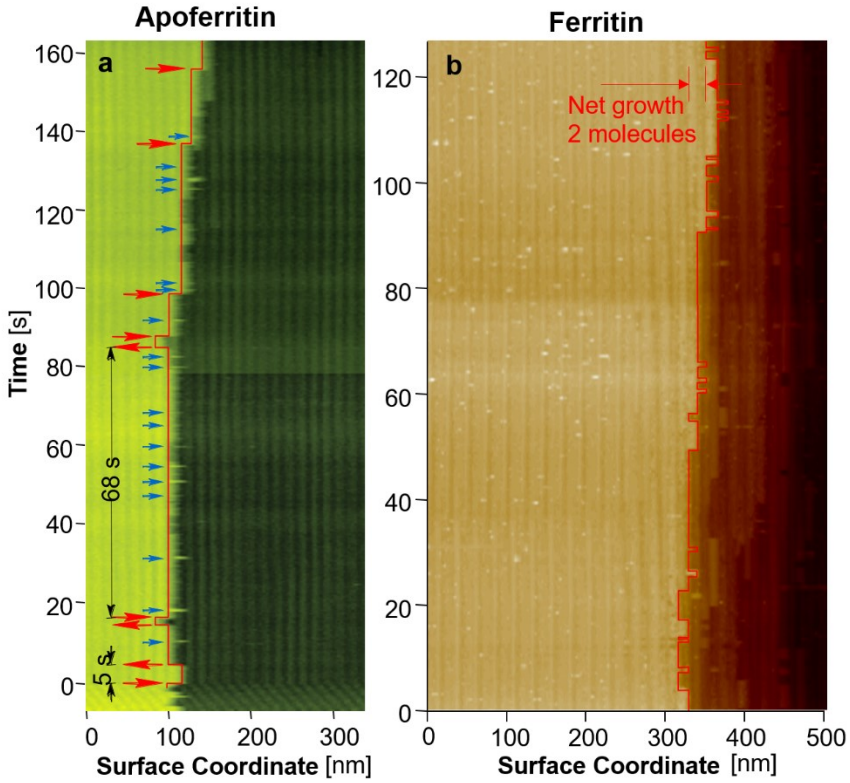

Fig. 6. The ratio between incoming and outgoing fluxes into a kink. Pseudoimages recorded in aqueous solutions with the scan axis parallel to the step disabled at time = 0, as in Refs. [16, 17]. **a.** Incorporation of molecules into apoferritin steps at (C/C_e – 1) = 2. Red contour and red arrows mark long-term attachment or detachment events. Blue arrows mark attachment followed by rapid detachment. **b.** Incorporation of molecules into ferritin steps at (C/C_e – 1) = 1. Red contour traces step position. Shifts of the red contour in a and b to the right correspond to molecules attaching to the monitored site, shifts to the left reflect detachments of molecules.

The ratio $j_+/j_- \leq 25/22 = 1.14$ for apoferritin and $j_+/j_- \leq 21/19 = 1.105$ for ferritin. The ≤ sign reflects the undetected pairs of attachment/detachment events separated by residence times shorter than the scanning period 0.5 s. These undetected events do not affect the measured net flux ($j+ - j-$). Additional attachment-detachment pairs detected by faster imaging, for instance, would contribute equally to both j_+ and j_- and bring the ratio j_+/j_- even lower. For both proteins, these ratios are much lower than the respective C/C_e and represent gross violations of the equality $j_+/j_- = C/C_e$ expected if molecules enter kinks directly from the solution. These violations cannot be attributed to depletion of the solution layer adjacent to the crystal—this factor becomes significant at ~ 100 × higher growth rates [82]—and suggest that the direct incorporation mechanism does not apply.

Direct imaging of solute molecules diffusing at the crystal surface.

A crucial issue for the validation of the surface diffusion pathway from the solution to the kinks is whether the solute molecules adsorbed on the crystal surface are mobile so that they can diffuse towards the kinks. Two sets of observations, with the proteins insulin and lysozyme [53, 83], reveal that molecules and even molecular assemblies migrate along the terraces between steps (Fig. 7).

AFM observations of single molecules adsorbed on crystal surfaces in solutions are rare or non-existent. Similar scanning probe techniques applied to metal and semiconductor surfaces held in ultra-high vacuum detect single adsorbed atoms and molecules only at very low temperatures, at which the surface mobility of the adsorbates reduces substantially [84]. Thus, the lack of direct sightings of molecules adsorbed on crystal surface may be due to their high mobility that makes them inaccessible to the relatively slow AFM scans and not to their absence from the surface.

Rhombohedral insulin crystals form in the islets of Langerhans in the pancreatic β-cells [85-88] with the function to protect the insulin from further proteolysis before secretion into the blood

serum [86, 87]. During growth of insulin crystals, the velocity of closely spaced steps, closer than 100 nm apart, is significantly slower than the velocity of well separated steps [89, 90]. The strength of this step-step interaction suggests that it is due to competition between the steps for supply of molecules adsorbed on the terraces between steps. Insulin molecules adsorbed on the terraces may be undetectable because of their mobility and hydrodynamic interactions with the scanning tip [80, 91]. Two-dimensional clusters, however, may have lower mobility due to their

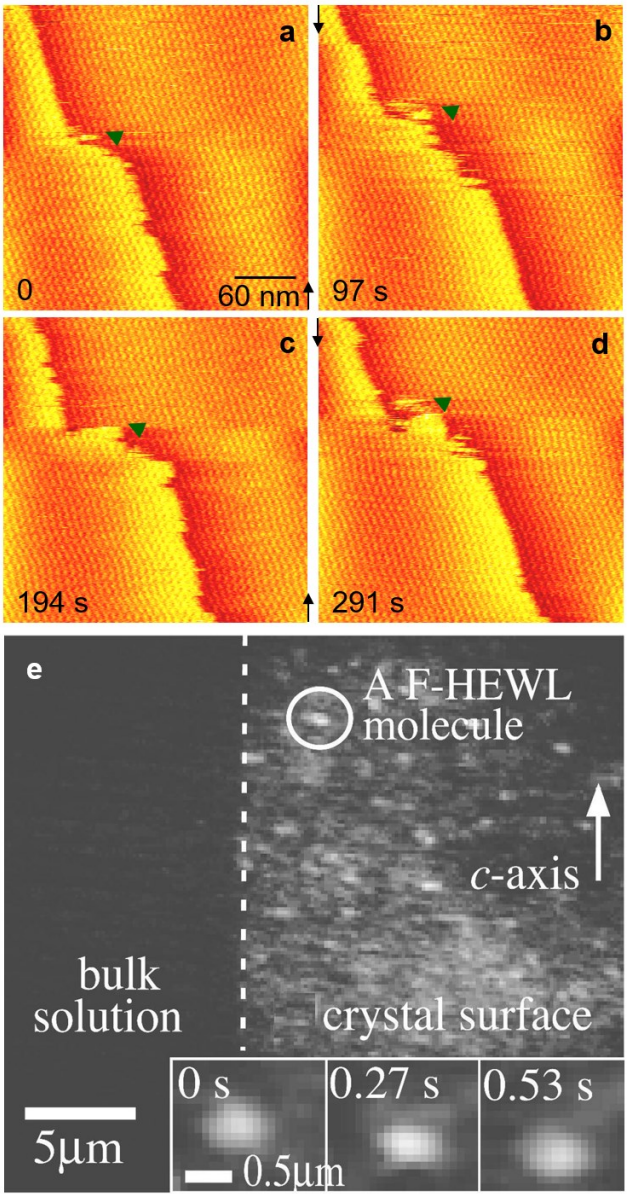

Fig. 7. The mobility of molecules and molecular assemblies in the adsorbed layer. **a – d.** The motion of two-dimensional (2D) clusters near steps on the surface of an insulin crystals grwoin

from an aqueous solution . Adapted from Ref. [53]. Copyright (2006) National Academy of Sciences. **a.** Starting configuration of a step. **b.** A 2D cluster, indicated with a white arrowhead. The image of the cluster is fuzzy likely due to cluster mobility. **c.** Cluster joins step creating a three- or four-molecule-deep mound. **d.** A second cluster indicated with a black arrowhead approaches protruding mound. Black arrows indicate scan directions. **e.** A single-molecule fluorescent microscopy image from *in situ* observation of a crystal of the protein lysozyme (HEWL) in an aqueous solution. Bright spots, highlighted with a circle, indicate individual fluorescently-labeled lysozyme molecules (F-HEWL). The insets show the motion of a F-HEWL molecule along the crystal surface. Adapted with permission from [83]. Copyright 2008 American Chemical Society.

larger size; how clusters may move along the surface is discussed in Refs. [92, 93]. The mobility of the clusters prevents identification of their structure prior to their association. They might be ordered or disordered, akin to a 2D liquid formed in the pool of hexamers adsorbed on the terraces: examples of liquid phases in two-dimensional systems have been discussed [94, 95]. In the vicinity of a step the cluster mobility seems to be further reduced and they are detected by AFM (Fig. 7a – e). A second cluster attaches to the protrusion created by association to the step of the first cluster (Fig. 7d).

Crystals of the protein lysozyme, readily purified from hen egg white and sometimes denoted as HEWL, have been a favorite model systems for fundamental studies of crystal growth [65, 96-103]. The strong dependence of the step velocity on the step-step separation has indicated that the lysozyme molecules reach the steps after adsorption on the terraces between them [64, 104]. Fluorescent microscopy imaging revealed that fluorescently-labeled lysozyme molecules (F-HEWL) accumulate at the solution crystal interface (Fig. 7e) and diffuse along the surface (Fig. 7e, insets) [83].

The direct incorporation pathway

Double height steps grow as fast as single height steps

The evidence that solute reaches the kinks directly from the solution expectedly emerges from the same experimental tests that were employed to examine the surface diffusion pathway. Particularly informative were the behaviors of steps on the surfaces of etioporphyrin I crystals growing from solutions in neat octanol. Single crystals of porphyrins and their metal derivatives

mostly have low symmetries and find potential use as organic semiconductors, solar cells, and field-effect transistors owing to their electronic and optical properties [105-107]. Time resolved *in situ* AFM measurements were used to compare the growth of steps as high as two lattice parameters to the growth of single-height steps. If solute reaches the steps via the crystal surface, the constrained solute supply stunts the growth of steps of double height. Concurrently, analytical models of step growth mediated by surface diffusion, Eq. (1), predict that v scales with h^{-1} [4, 48, 66]. By contrast, if the steps feed directly from the solution, the supply field is three-dimensional and abundant for twinned steps. Closed-form expressions for this growth mode, Eq. (4), predict negligible $v(h)$ correlation [2, 8]. The AFM measurements reveal that the velocities of steps as high as two lattice parameters are close to those of steps of single height (Fig. 8). The comparable rates of growth of twinned and single-height steps affirm that steps on etioporphyrin I prefer the direct incorporation pathway.

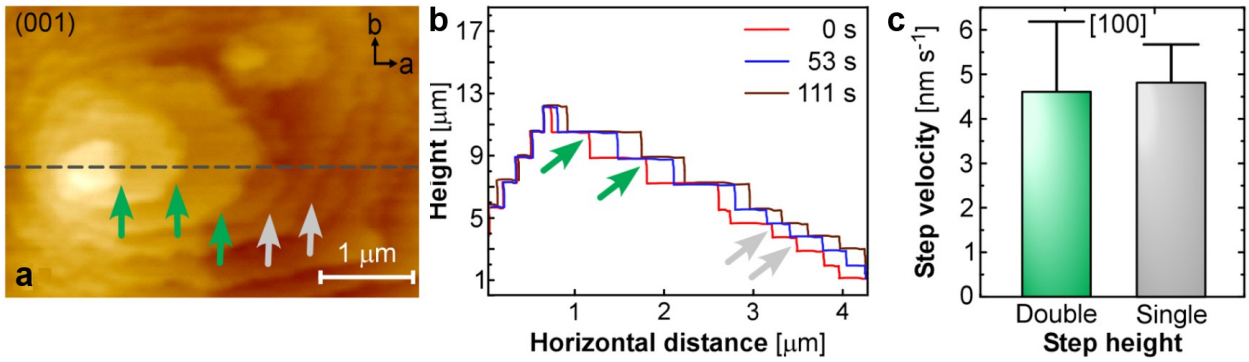

Fig. 8. Growth of single and double height steps on a (001) face of an etioporphyrin I crystal growing from a solution in neat octanol at C = 0.25 mM.. **a.** An AFM image of the growth of single (silver arrows) and double (green arrows) height steps of a (010) face **b.** The evolution of the surface profile along the dotted line in a. **c.** Comparison of the average velocities of single and double height steps. Error bars represent the standard deviations from the averages over measurements of 10 double and 10 single height steps. Reproduced from [56] with permission from the Royal Society of Chemistry.

Step density does not affect step velocity

Additional evidence that the steps on etioporphyrin I crystals feed directly from the solution comes from the lack of dependence of the step velocity on the separation between steps (Fig. 9). Steps separated by as little as 20 nm grow as fast as steps that are more than 800 nm apart. The

fast growth rates of closely spaced steps certify the lack of competition for supply between them, typical of the direct incorporation pathway. Unpublished results from the Vekilov laboratory indicate that etioporphyrin I crystals select the direct incorporation pathway to supply solute to the steps not only during growth from octanol, but also from hexanol, butanol, and DMSO.

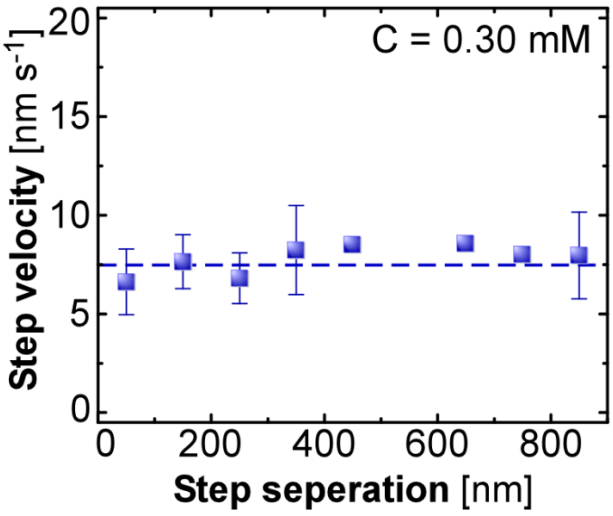

Fig. 9. The velocity of steps on the (001) face of etioporphyrin I crystals growing from a solution in neat octanol does not correlate with the step separation l. C = 0.30 mM. The averages of 15 measurements for each 100 nm wide l range, are shown. Vertical error bars represent the standard deviation of each such group of data.

What determines the selection of the molecular pathway to the steps?

The cases discussed above appear to suggest one important distinction between the crystallization systems that prefer the surface diffusion pathway and those whose steps feed directly from the solution. The ionic, organic, protein, and biomineral crystals that employ the surface diffusion pathway all grow from either purely aqueous, or, in the cases of hematin and olanzapine, mixed aqueous-organic solvents. By contrast, etioporphyrin I crystals grow from a purely organic solvent and select direct solute incorporation.

Why would water-rich solvents encourage solute supply to the steps via the crystal surface? We tentatively posit that this is because of the lower activation barrier for surface diffusion on a surface in contact with water-containing solvents. These lower barriers accelerate molecular

migration, extend the characteristic surface diffusion length, and contribute to abundant solute supply to the kinks from the surface. In turn, strong surface fluxes provide for faster step growth using this pathway than using the direct incorporation pathway. Water uniquely binds to both polar and nonpolar patches on the crystal surfaces by Coulomb, polar, van der Waals, hydrogen, and structural bonds; the same forces support complexation between solvent water and the solute molecules (Fig. 10a, stage 1) [108-111]. A water envelope around hematin solute molecules and

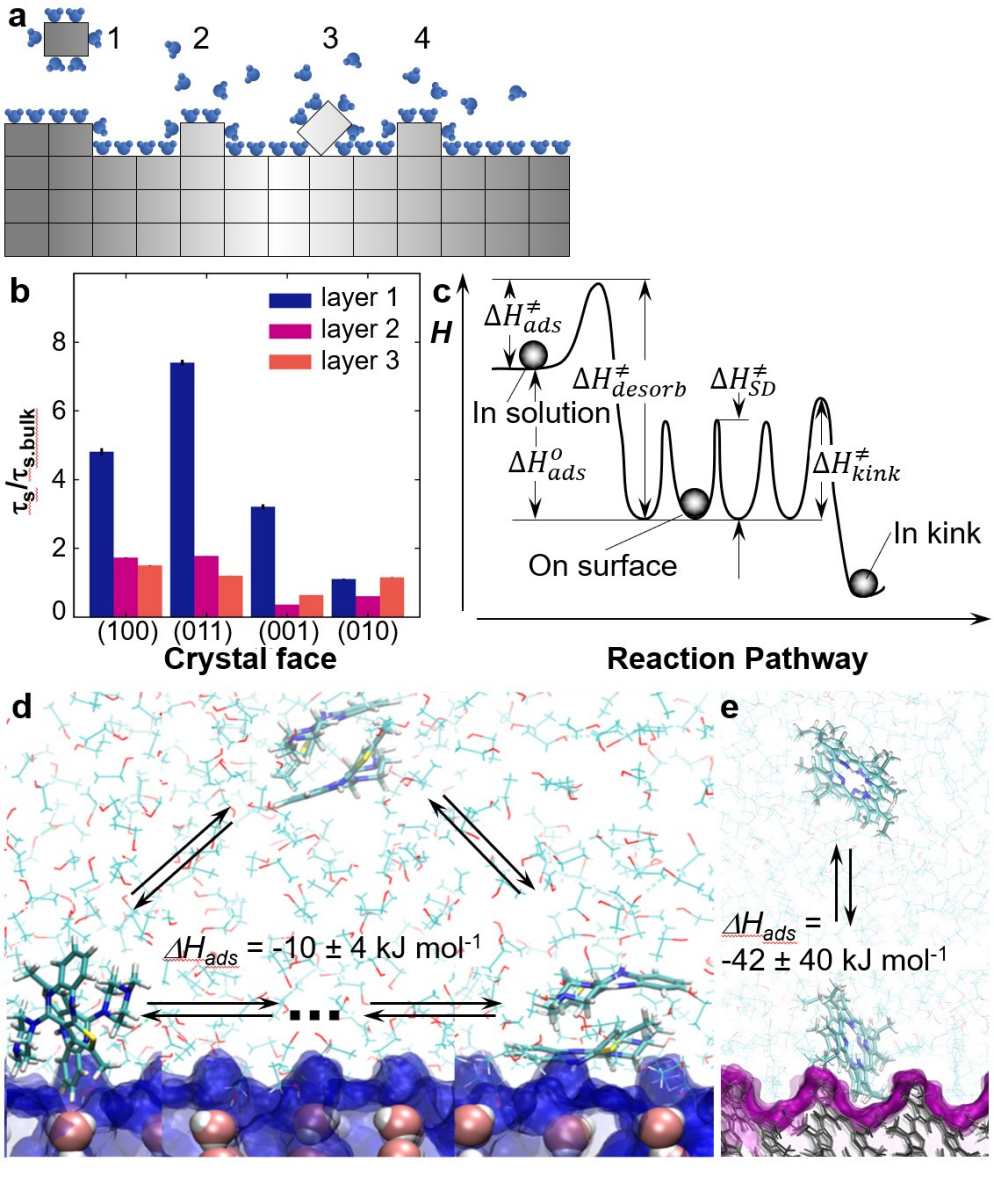

Fig. 10. The energetics of surface diffusion. a. Schematic illustration of water molecules associating to solutes and crystal surfaces at four stages of adsorption. 1, solute molecule in the

solution; 2, solute adsorbs on the surface, leading to the release of solvent molecules; 3, adsorbed solute molecule breaks some contacts with surface *en route* to an adjacent adsorption site; 4; adsorbed molecule at a new adsorption site. **b.** Survival times τ_s of solvent molecules in three layers parallel to (100), (011), (001) and (010) faces of β-hematin crystals normalized by the bulk value $\tau_{s,\mathrm{bulk}} \approx 8.1$ ps. Adapted with permission from [112]. Copyright 2008 American Chemical Society. **c.** Enthalpy variation along the reaction coordinate for the surface diffusion mechanism. $\Delta H^{\neq}_{ads}$, $\Delta H^{\neq}_{desorb}$, $\Delta H^{\neq}_{SD}$, $\Delta H^{\neq}_{kink}$ are the activation barriers for, respectively, adsorption, desorption, surface diffusion, and incorporation into kinks from the surface. The equilibrium enthalpy of adsorption $\Delta H^{o}_{ads} = \Delta H^{\neq}_{ads} - \Delta H^{\neq}_{des}$. **d, e.** MD simulations of adsorption of an olanzapine dimer on the (002) face of an olanzapine crystal in contact with a 1:1 ethanol water mixture, in **d**, adapted with permission form [54], and of an etioporphyrin I dimer on a (001) face of an etioporphyrin I crystal in contact with octanol in **e**. Molecules in both crystals are represented with their solvent accessible surfaces. In the solution, ethanol and octanol molecules are shown as thin sticks; solvent waters in **d** are omitted for clarity. Solute dimers in the solution and at the surface are shown as thick sticks. Only two of the numerous surface configurations of the adsorbed dimers are shown in **d** and only one in **e**. ΔH^{o}_{ads} is evaluated as the difference between the averaged enthalpies of dimers on the crystal surface and in the solution bulk.

along the surface of β-hematin crystals has been demonstrated in a solution that only contains 5 volume % water (Fig. 10b) [112]. When a solute molecule adsorbs on the surface, the free energy gain due to the formation of bonds with the surface molecules is partially offset by the loss of the free energy of the broken bonds with the water coating both solute and surface (Fig. 10a, stage 2). As a result, the adsorption energy is lower in aqueous or partially aqueous solvents than it would be in a water-free solvent.

To migrate along the surface, a solute molecule breaks some of the bonds with the surface, while retaining others (Fig. 10 a, stage 3). Saturating the briefly opened valencies with water lowers the energy of the intermediate state between two adsorption sites (Fig. 10 a, position 3), which represents the activation barrier for surface diffusion, $\Delta H^{\neq}_{SD}$. (Fig. 10c).

The interaction of organic solvents with the solute and the crystal surface is largely constrained to van der Waals forces [113], whose disruption upon solute adsorption on the surface weakens the adsorption bonds much less than the release of water. Thus, the adsorption energy and the related activation barrier for surface diffusion remain high, suppressing solute migration along the surface and the flux of molecules towards the kinks.

To validate this scenario would require experimental determination of $\Delta H_{SD}^{\neq}$, or at least of the related $\Delta H_{desorb}^{\neq}$, in both water-rich and water-free solvents. Unfortunately, neither $\Delta H_{SD}^{\neq}$ nor $\Delta H_{desorb}^{\neq}$ have been directly measured. Indirect evaluation from kinetic data may be unreliable owing to the complex dynamics of solute-solvent structures held together by a variety of bonds. Furthermore, estimating kinetic barriers by molecular dynamics simulations is challenged by the multiple trajectories that an adsorbed solute may take on the way to another adsorption site or back into the solution. A more feasible approach is to numerically evaluate the equilibrium adsorption enthalpy $\Delta H_{ads}^{o} = \Delta H_{ads}^{\neq} - \Delta H_{desorb}^{\neq}$ and use it as an approximate measure for $\Delta H_{SD}^{\neq}$ (Fig. 10c).

We employed all-atom MD simulations to evaluate the equilibrium enthalpy ΔH_{ads}^{o} of adsorption of olanzapine dimers on a (002) face of olanzapine crystals in contact with a 1:1 mixture of ethanol and water [54] and of etioporphyrin dimers on the (001) face of etioporphyrin I crystals in contact with pure octanol [55, 56]. Both the (002) faces of olanzapine and (001) faces of etioporphyrin I grow by incorporation of solute dimers that exist in equilibrium with a majority of monomers [55, 56]. The olanzapine steps feed from solute adsorbed in the crystal surface (Fig. 5c) [54]. By contrast, solute reaches etioporphyrin I steps directly from the solution (Fig. 8) [56].

The MD results reveal that the adsorption enthalpy is -10±4 kJ mol^{-1} for olanzapine dimers in an ethanol water mixture (Fig. 10 d) and -42±40 kJ mol^{-1} for etioporphyrin I dimers in neat octanol (Fig. 10e). The large uncertainty of both enthalpy values is due to the limited numbers of trajectories (ca 70) considered in the highly computer-time intensive all-atom evaluations [56]. Importantly, the enthalpy of adsorption from a purely organic solvent is substantially greater than that from a partially aqueous solvent. We attribute the lower ΔH_{ads}^{o} in the mixed solvent to the water molecules that associate to both crystal surface and the solute molecules and stabilize the desorbed state (Fig. 10a). Assuming that ΔH_{ads}^{o} correlates with $\Delta H_{SD}^{\neq}$ (Fig. 10c), the greater ΔH_{ads}^{o} in neat octanol suggest that $\Delta H_{SD}^{\neq}$ is much higher. The higher barrier for surface diffusion in

octanol would powerfully suppress surface diffusion and the surface flux towards kinks, promoting direct incorporation to the faster preferred pathway from the solution to the steps.

Notably, the discrimination between the two step supply pathways may not require such drastic differences in solute adsorption energy as seen between the (002) face of olanzapine and (001) face of etioporphyrin I. Unpublished results of the Vekilov and Palmer groups reveal that the solute adsorption enthalpy on the (010) face of etioporphyrin I crystals is ca. -26 kJ mol^{-1}, which appears sufficient to bolster direct incorporation into steps on that face [56].

Summary and conclusions

The experimental results reviewed here indicate that ionic, organic, protein, and biomineral crystals that employ the surface diffusion pathway all grow from either purely aqueous or mixed aqueous-organic solvents. Purely organic solvents appear to select direct solute incorporation.

The MD results with olanzapine and etioporphyrin I tentatively support a criterion for the selection of the pathway from the solution to the steps based on the interactions of the solvent with solute and the crystal surface. Solvents that strongly associate to the solute and the crystal surfaces weaken the solute adsorption on the terraces. The weaker adsorption contributes to faster surface diffusion and, somewhat counterintuitively, to abundant solute supply to the steps, which in turn makes solute supply *via* the surface diffusion pathway faster than directly from the solution.

Solvents that do not attenuate the solute-crystal surface attraction promote strong adsorption, which may strongly suppress surface diffusion and the solute supply to the steps *via* the crystal surface. Such solvents may encourage direct incorporation into the kinks.

Computational efforts to predict *a priori* the pathway from the solution to the surface may not necessarily be limited to time-intensive all-atom MD simulations. Coarse-grained methods may be able to tackle this task if they are not constrained to only considering bulk solvent

properties and faithfully account for solvent association to the crystal surfaces and to solute molecules.

Acknowledgements

Over the years, we have greatly benefitted from discussions of how solute molecules reach the steps with a line of colleagues. Alex Chernov spurred the initial interest in the issue. R. Kaischew, F. Rosenberger, J. Rimer, K. Tsukamoto, G. Sazaki, M. Maruyama, J. De Yoreo, T. Land, M. Sleutel, D. Maes, J. Lutsko, E. Vlieg, and many others helped to straighten our arguments. Former students and postdocs who worked on the results presented here include S.-T. Yau, N. Booth, K. Chen, D. Georgiou, O. Gliko, I. Reviakine, K. Newlin (Olafson), and W. Ma. Our work on solution crystallization has been generously funded by NSF (Grants ## DMR 2128121 and DMR-1710354), NIH (Grants ## R01 AI150763 and 1R21AI126215), and NASA (Grants ## NNX14AD68G and NNX14AE79G), to whom we are immensely grateful.

References

[1] W.K. Burton, Cabrera, N. &. Frank, F.C., The growth of crystals and equilibrium structure of their surfaces., *Phil. Trans. Roy. Soc. London Ser. A*, **243** (1951) 299- 360.
[2] A.A. Chernov, The spiral growth of crystals, Sov. Phys. Uspekhi, 4 (1961) 116-148.
[3] P. Bennema, Analysis of crystal growth models for slightly supersaturated solutions, J. Crystal Growth, 1 (1967) 278-286.
[4] G.H. Gilmer, R. Ghez, N. Cabrera, An analysis of combined volume and surface diffusion processes in crystal growth, J. Crystal Growth, 8 (1971) 79-93.
[5] P. Dandekar, Z.B. Kuvadia, M.F. Doherty, Engineering Crystal Morphology, Annual Review of Materials Research, 43 (2013) 359-386.
[6] M.N. Joswiak, M.F. Doherty, B. Peters, Ion dissolution mechanism and kinetics at kink sites on NaCl surfaces, Proceedings of the National Academy of Sciences of the United States of America, 115 (2018) 656-661.
[7] M.A. Lovette, A.R. Browning, D.W. Griffin, J.P. Sizemore, R.C. Snyder, M.F. Doherty, Crystal Shape Engineering, Industrial & Engineering Chemistry Research, 47 (2008) 9812-9833.
[8] A.A. Chernov, Modern Crystallography III, Crystal Growth,, Springer, Berlin, 1984.
[9] P.G. Vekilov, Y.G. Kuznetsov, A.A. Chernov, Interstep interaction in solution growth; (101) ADP face., J. Crystal Growth, 121 (1992) 643-655.
[10] P.G. Vekilov, Y.G. Kuznetsov, A.A. Chernov., The effect of temperature on step motion; (101) ADP face, J. Crystal Growth, 121 (1992) 44-52.
[11] E.D. Williams, N.C. Bartelt, Thermodynamics of surface morphology, *Science*, **251** (1991) 393-400.
[12] A.A. Chernov, Theory of stability of faceted forms of crystals, Sov. Phys. -Crystallogr., 16 (1972) 734-750.

[13] A.A. Chernov, Stability of faceted crystal shapes, J. Crystal Growth, 24/25 (1974) 11-31.
[14] C.N. Nanev, Instability of faceted crystal shapes, Cryst. Reports, 3 (1993) 1-74.
[15] P.G. Vekilov, L.A. Monaco, F. Rosenberger, Facet morphology response to non-uniformities in nutrient and impurity supply. I. Experiments and interpretation., J. Crystal Growth, 156 (1995) 267-278.
[16] H. Lin, P.G. Vekilov, F. Rosenberger, Facet morphology response to non-uniformities in nutrient and impurity supply. II. Numerical modeling., J. Crystal Growth, 158 (1996) 552-559.
[17] J. Desarnaud, H. Derluyn, J. Carmeliet, D. Bonn, N. Shahidzadeh, Hopper Growth of Salt Crystals, The Journal of Physical Chemistry Letters, 9 (2018) 2961-2966.
[18] I. Sunagawa, P. Bennema, Modes of Vibrations in Step Trains: Rhythmical Bunching, J. Cryst. Growth, 46 (1979) 451-450.
[19] S.R. Coriell, B.T. Murrary, A.A. Chernov, G.B. McFadden, Step bunching on a vicinal face of a crystal growing in a flowing solution, J. Crystal Growth, 169 (1996) 773-785.
[20] J.P. Van der Eerden, H. Mueller-Krumbhaar, Dynamic Coarsening of Crystal Surfaces by Formation of Macrosteps, Physical Review Letters, 57 (1986) 2431-2433.
[21] P.G. Vekilov, F. Rosenberger, Intrinsic kinetics fluctuations as cause of growth inhomogeneity in protein crystals, Phys. Rev**.** E, 57 (1998) 6979-6981.
[22] E. Bauser, Atomic Mechanisms in Semiconductor Liquid Phase Epitaxy, in: D.T.J. Hurle (Ed.) Handbook of Crystal Growth, North Holland, Amsterdam, 1994, pp. 879-911.
[23] A.A. Chernov, I.L. Smol'skii, V.F. Parvov, Y.G. Kuznetsov, V.N. Rozhanskii, X-ray diffraction investigation of the growth of ADP crystals, Sov. Phys. Crystallogr., 25 (1980) 469-474.
[24] A.A. Chernov, T. Nishinaga, Stability of uniform step patterns, in: I. Sunagawa (Ed.) Materials Science of the Earth's Interior, Terra, Tokyo, 1984, pp. 207-255.
[25] A.A. Chernov, Y.G. Kuznetsov, I.L. Smol'sky, V.N. Rozhanskii, Hydrodynamic effects in the growth of ADP crystals from aqueous solutions in the kinetic regime, Sov. Phys Crystallogr, 31 (1986) 705-711.
[26] A.A. Chernov, How does flow within the boundary layer influence the morphological stability?, J. Crystal Growth, 118 (1992) 333-347.
[27] A.A. Chernov, Coreill, S. R., Murray, B.T., Kinetic Self-Stability of a Stepped Interface: Growth Into a Supercooled Melt, J. Cryst. Growth, 149 (1995) 120-130.
[28] S.R. Coriell, B.T. Murray, A.A. Chernov, Kinetic self-stabilization of a stepped interface: Growth into a supercooled melt, J. Cryst. Growth, 149 (1995) 120-130.
[29] S.R. Coriell, A.A. Chernov, B.T. Murray, G.B. McFadden, Step bunching: generalized approach, J. Crystal Growth, 183 (1998) 669-682.
[30] A.A. Chernov, L.N. Rashkovich, I.V. Yamlinski, N.V. Gvozdev, Kink kinetics, exchange fluxes, 1D "nucleation" and adsorption on the (010) face of orthorhombic lysozyme crystals, J. Phys.:Condens. Matter, 11 (1999) 9969-9984.
[31] B.T. Murray, S.R. Coriell, A.A. Chernov, G.B. McFadden, The effect of oscillatory shear flow on step bunching, Journal of Crystal Growth, 218 (2000) 434-446.
[32] N.A. Booth, A.A. Chernov, P.G. Vekilov, Characteristic lengthscales of step bunching in KDP crystal growth: in-situ differential phase-shifting interferometry study., J. Crystal Growth, 237-239 (2002) 1818-1824.
[33] N.A. Booth, A.A. Chernov, P.G. Vekilov, Step Bunching in KDP Crystal Growth: Phenomenology, J. Materials Research, 17 (2002) 2059-2065.
[34] F.C. Frank, On the kinmatic theory of crystal growth and dissolution processes, in: R.H. Doremus, B.W. Roberts, D. Turnbul (Eds.) Growth and Perfection of Crystals, Wiley, New York, 1958, pp. 411-417.
[35] S. Stoyanov, V. Tonchev, Properties and dynamic interaction of step density waves at a crystal surface during electromigration affected sublimation, Phys. Rev. B, 58 (1998) 1590-1600.
[36] A. Pimpinelli, V. Tonchev, A. Videcoq, M. Vladimirova, Scaling and Universality of Self-Organized Patterns on Unstable Vicinal Surfaces, Phys. Rev. Lett, 88 (2002) 206103.

[37] R. Kaischew, Zur Theorie des Kristallwaschstums, *Z. Phys.*, **102** (1936) 684-690.
[38] M. Volmer, Kinetik der Phasenbildung, Steinkopff, Dresden, 1939.
[39] I.N. Stranski, Zur Theorie des Kristallwachstums, Z. Phys. Chem., 136 (1928) 259-278.
[40] S.-T. Yau, D.N. Petsev, B.R. Thomas, P.G. Vekilov, Molecular-level thermodynamic and kinetic parameters for the self-assembly of apoferritin molecules into crystals., J. Mol. Biol., 303 (2000) 667-678.
[41] S.-T. Yau, B.R. Thomas, P.G. Vekilov, Molecular mechanisms of crystallization and defect formation, Phys. Rev. Lett., 85 (2000) 353-356.
[42] D.N. Petsev, K. Chen, O. Gliko, P.G. Vekilov, Diffusion-limited kinetics of the solution-solid phase transition of molecular substances, Proc. Natl. Acad. Sci. USA, 100 (2003) 792-796.
[43] M.A. Lovette, M.F. Doherty, Multisite models to determine the distribution of kink sites adjacent to low-energy edges, Physical Review E, 85 (2012) 021604.
[44] P.G. Vekilov, Y.G. Kuznetsov, A.A. Chernov, Dissolution morphology and kinetics of (101) ADP face; mild etching of surface defects., J. Crystal Growth, 102 (1990) 706-716.
[45] J.J. De Yoreo, P.G. Vekilov, Principles of crystal nucleation and growth, in: Biomineralization, 2003, pp. 57-93.
[46] P.G. Vekilov, Incorporation at kinks: kink density and activation barriers, , in: M. Skowronski, J.J. DeYoreo, C.A. Wang (Eds.) Perspectives on Inorganic, Organic and Biological Crystal Growth: From Fundamentals to Applications: AIP Conference Proceedings, AIP, Melville, NY, 2007, pp. 235-267.
[47] P.G. Vekilov, What determines the rate of growth of crystals from solution? , Crystal Growth and Design,, 7 (2007) 2796-2810.
[48] K.N. Olafson, M.A. Ketchum, J.D. Rimer, P.G. Vekilov, Mechanisms of hematin crystallization and inhibition by the antimalarial drug chloroquine, Proceedings of the National Academy of Sciences, 112 (2015) 4946-4951.
[49] K.N. Olafson, M.A. Ketchum, J.D. Rimer, P.G. Vekilov, Molecular Mechanisms of Hematin Crystallization from Organic Solvent, Crystal Growth & Design, 15 (2015) 5535-5542.
[50] K.N. Olafson, J.D. Rimer, P.G. Vekilov, Early Onset of Kinetic Roughening due to a Finite Step Width in Hematin Crystallization, Physical Review Letters, 119 (2017) 198101.
[51] V.V. Voronkov, The movement of an elementary step by means of the formation of one-dimensional nuclei., Sov. Phys.-Crystallogr., 15 (1970) 8-13.
[52] H.H. Teng, P.M. Dove, J.J. De Yoreo, Kinetics of calcite growth: Surface processes and relationships to macroscopic rate laws, Geochimica Et Cosmochimica Acta, 64 (2000) 2255-2266.
[53] D.K. Georgiou, P.G. Vekilov, A fast response mechanism for insulin storage in crystals may involve kink generation by association of 2D clusters, Proc. Natl. Acad. Sci. USA, 103 (2006) 1681-1686.
[54] M. Warzecha, L. Verma, B.F. Johnston, J.C. Palmer, A.J. Florence, P.G. Vekilov, Olanzapine crystal symmetry originates in preformed centrosymmetric solute dimers, Nature Chemistry, 12 (2020) 914-920.
[55] L. Verma, M. Warzecha, R. Chakrabarti, V.G. Hadjiev, J.C. Palmer, P.G. Vekilov, How to Identify the Crystal Growth Unit, Israel Journal of Chemistry, 61 (2021) 818-827.
[56] M. Warzecha, L. Verma, R. Chakrabarti, V.G. Hadjiev, A.J. Florence, J.C. Palmer, P.G. Vekilov, Precrystallization solute assemblies and crystal symmetry, Faraday Discussions, (2022).
[57] M. Maruyama, K. Tsukamoto, G. Sazaki, Y. Nishimura, P.G. Vekilov, Chiral and Achiral Mechanisms of Regulation of Calcite Crystallization, Crystal Growth & Design, 9 (2009) 127-135.
[58] V.G. Levich, Physicochemical Hydrodynamics, Prentice Hall, Englewood Cliffs, 1962.
[59] K.N. Olafson, T.Q. Nguyen, J.D. Rimer, P.G. Vekilov, Antimalarials inhibit hematin crystallization by unique drug–surface site interactions, Proceedings of the National Academy of Sciences, 114 (2017) 7531-7536.
[60] W. Ma, J.F. Lutsko, J.D. Rimer, P.G. Vekilov, Antagonistic cooperativity between crystal growth modifiers, Nature, 577 (2020) 497-501.

[61] D.E. Goldberg, A.F. Slater, A. Cerami, G.B. Henderson, Hemoglobin degradation in the malaria parasite Plasmodium falciparum: an ordered process in a unique organelle, Proceedings of the National Academy of Sciences, 87 (1990) 2931-2935.
[62] R.G. Ridley, Medical need, scientific opportunity and the drive for antimalarial drugs, Nature, 415 (2002) 686-693.
[63] S. Pagola, P.W. Stephens, D.S. Bohle, A.D. Kosar, S.K. Madsen, The structure of malaria pigment β-haematin, Nature 404 (2000) 307-310.
[64] P.G. Vekilov, H. Lin, F. Rosenberger, Unsteady crystal growth due to step-bunch cascading, Phys. Rev. E, 55 (1997) 3202-3214.
[65] P.G. Vekilov, J.I.D. Alexander, F. Rosenberger, Nonlinear response of layer growth dynamics in the mixed kinetics-bulk transport regime, Phys. Rev. E, 54 (1996) 6650-6660.
[66] T.A. Land, J.J. DeYoreo, J.D. Lee, An in-situ AFM investigation of canavalin crystallization kinetics, Surf. Sci., 384 (1997) 136-155.
[67] M. Sleutel, R. Willaert, C. Gillespie, C. Evrard, L. Wyns, D. Maes, Kinetics and Thermodynamics of Glucose Isomerase Crystallization, Crystal Growth & Design, 9 (2009) 497-504.
[68] M. Sleutel, C. Vanhee, C.V. de Weerdt, K. Decanniere, D. Maes, L.W.R. Willaert, The role of surface diffusion in the growth mechanism of triosephosphate isomerase crystals, Crystal Growth & Design, 8 (2008) 1173-1180.
[69] K. Chen, P.G. Vekilov, Evidence for the surface diffusion mechanism of solution crystallization from molecular-level observations with ferritin, Phys. Rev. E, 66 (2002) 021606.
[70] M. Likhatski, A. Karacharov, A. Kondrasenko, Y. Mikhlin, On a role of liquid intermediates in nucleation of gold sulfide nanoparticles in aqueous media, Faraday Discussions, 179 (2015) 235-245.
[71] G. Ehrlich, F.G. Hudda, Asymetric capture at steps, J. Chem. Phys., 44 (1966) 1039-1052.
[72] R.L. Schwoebel, E.J. Shipsey, Step motion on crystal surfaces, J. APpl. Phys., 37 (1966) 3682-3686.
[73] B. Fulton, K.L. Goa, Olanzapine, Drugs, 53 (1997) 281-298.
[74] R.M. Bhardwaj, L.S. Price, S.L. Price, S.M. Reutzel-Edens, G.J. Miller, I.D.H. Oswald, B.F. Johnston, A.J. Florence, Exploring the Experimental and Computed Crystal Energy Landscape of Olanzapine, Crystal Growth & Design, 13 (2013) 1602-1617.
[75] W.H. Massover, Ultrastructure of ferritin and apoferritin: a review, Micron, 24 (1993) 389-437.
[76] S. Gider, D.D. Awschalom, T. Douglas, S. Mann, M. Chaparala, Classical and quantum magnetic phenomena in natural and artificial ferritin proteins [see comments], Science, 268 (1995) 77-80.
[77] D. Yang, K. Nagayama, Permeation of small molecules into the cavity of ferritin as revealed by proton nuclear magnetic resonance relaxation, Biochem J, 307 (1995) 253-256.
[78] D.N. Petsev, B.R. Thomas, S.-T. Yau, D. Tsekova, C. Nanev, W.W. Wilson, P.G. Vekilov, Temperature-independent Solubility and Interactions between Apoferritin Monomers and Dimers in Solution, J. Crystal Growth, 232 (2001) 21-29.
[79] D.N. Petsev, B.R. Thomas, S.-T. Yau, P.G. Vekilov, Interactions and Aggregation of Apoferritin Molecules in Solution: Effects of Added Electrolytes, Biophysical J., 78 (2000) 2060-2069.
[80] S.-T. Yau, B.R. Thomas, O. Galkin, O. Gliko, P.G. Vekilov, Molecular mechanisms of microheterogeneity-induced defect formation in ferritin crystallization, Proteins: Structure, Function, Genetics, 43 (2001) 343-352.
[81] S.-T. Yau, B.R. Thomas, P.G. Vekilov, Real time, in-situ, monitoring of apoferritin crystallization and defect formation with molecular resolution., J. Crystal Growth, 232 (2001) 188-194.

[82] H. Lin, D.N. Petsev, S.-T. Yau, B.R. Thomas, P.G. Vekilov, Lower Incorporation of Impurities in Ferritin Crystals by Suppression of Convection: Modeling Results, Crystal Growth and Design, 1 (2001) 73-79.
[83] G. Sazaki, M. Okada, T. Matsui, T. Watanabe, H. Higuchi, K. Tsukamoto, K. Nakajima, Single-Molecule Visualization of Diffusion at the Solution−Crystal Interface, Crystal Growth & Design, 8 (2008) 2024-2031.
[84] A. Bogicevic, S. Ovesson, P. Hyldgaard, B.I. Lundqvist, H. Brune, D.R. Jennison, Nature, Strength, and Consequences of Indirect Adsorbate Interactions on Metals, Physical Review Letters, 85 (2000) 1910-1913.
[85] S. Howell, M. Tyhurst, The insulin storage granule, in: Poisner, Trifaro (Eds.) The secretory granule, Elsevier, Amsterdam, 1982, pp. 155-172.
[86] G. Dodson, D. Steiner, The role of assembly in insulin's biosynthesis, Current Opinion in Structural Biology, 8 (1998) 189-194.
[87] P. Halban, R. Mutkoski, G. Dodson, L. Orci, Resistance of the insulin crystal to lysosomal proteases: implications for pancreatic B-cell crinophagy, Diabetologia, 30 (1987) 348-353.
[88] E.N. Baker, T.L. Blundell, J.F. Cutfield, S.M. Cutfield, E.J. Dodson, G.G. Dodson, D.M. Crowfoot-Hodgkin, R.E. Hubbard, N.W. Isaacs, C.D. Reynolds, K. Sakabe, N. Sakabe, N.M. Vijayan, The Structure of 2Zn Pig Insulin Crystals at 1.5A Resolution, Phil.Trans.R.Soc.Lond., B319 (1988) 369-456.
[89] I. Reviakine, D.K. Georgiou, P.G. Vekilov, Capillarity effects on the crystallization kinetics: insulin., J. Am. Chem. Soc., 125 (2003) 11684-11693.
[90] O. Gliko, I. Reviakine, P.G. Vekilov, Stable Equidistant Step Trains during Crystallization of Insulin, Phys. Rev. Lett, 90 (2003) 225503.
[91] D.E. Hooks, C.M. Yip, M.D. Ward, Nanoconfined Electrochemical Nucleation of Crystalline Molecular Monolayers on Graphite Substrates, J. Phys. Chem. B, 102 (1998) 9958-9965.
[92] G.L. Kellogg, Oscillatory Behavior in the Size Dependence of Cluster Mobility on Metal Surfaces: Rh on Rh(100), Phys. Rev. Lett., 73 (1994) 1833–1836.
[93] D.S. Sholl, R.T. Skodje, Diffusion of Clusters of Atoms and Vacancies on Surfaces and the Dynamics of Diffusion-Driven Coarsening, Phys. Rev. Lett., 75 (1995) 3158–3161.
[94] I. Lyuksyutov, A.G. Naumovets, V. Pokrovsky, Two-Dimensional Crystals, Academic Press, Boston, 1992.
[95] D.K. Schwartz, Mechanisms and kinetics of self-assembled monolayer formation, Annual Review of Physical Chemistry, 52 (2001) 107-137.
[96] S.D. Durbin, W.E. Carlson, Lysozyme crystal growth studied by atomic force microscopy, J. Crystal Growth, 122 (1992) 71-79.
[97] S.D. Durbin, G. Feher, Studies of crystal growth mechanims of proteins by electron microscopy, J. Mol. Biol., 212 (1990) 763-774.
[98] P. Dold, E. Ono, K. Tsukamoto, G. Sazaki, Step velocity in tetragonal lysozyme growth as a function of impurity concentration and mass transport conditions, J. Cryst. Growth, 293 (2006) 102-109.
[99] A.E.S. Van Driessche, G. Sazaki, F. Otalora, F.M. Gonzalez-Rico, P. Dold, K. Tsukamoto, K. Nakajima, Direct and Noninvasive Observation of Two-Dimensional Nucleation Behavior of Protein Crystals by Advanced Optical Microscopy, Crystal Growth & Design, 7 (2007) 1980-1987.
[100] T. Yamazaki, Y. Kimura, P.G. Vekilov, E. Furukawa, M. Shirai, H. Matsumoto, A.E.S. Van Driessche, K. Tsukamoto, Two types of amorphous protein particles facilitate crystal nucleation, Proceedings of the National Academy of Sciences, 114 (2017) 2154-2159.
[101] D. Maes, M.A. Vorontsova, M.A.C. Potenza, T. Sanvito, M. Sleutel, M. Giglio, P.G. Vekilov, Do protein crystals nucleate within dense liquid clusters?, Acta Crystallographica Section F, 71 (2015) 815-822.

[102] V. Stojanoff, D.P. Siddons, L.A. Monaco, P.G. Vekilov, F. Rosenberger, X-ray topography of tetragonal lysozyme grown by the temperature controlled technique., Acta Crystallogr. Section D, 53 (1997) 588-595.
[103] Y. Li, V. Lubchenko, M.A. Vorontsova, L. Filobelo, P.G. Vekilov, Ostwald-Like Ripening of the Anomalous Mesoscopic Clusters in Protein Solutions, The Journal of Physical Chemistry B, 116 (2012) 10657-10664.
[104] P.G. Vekilov, F. Rosenberger, Dependence of lysozyme growth kinetics on step sources and impurities, J. Crystal Growth, 158 (1996) 540-551.
[105] C.-M. Che, H.-F. Xiang, S.S.-Y. Chui, Z.-X. Xu, V.A.L. Roy, J.J. Yan, W.-F. Fu, P.T. Lai, I.D. Williams, A High-Performance Organic Field-Effect Transistor Based on Platinum(II) Porphyrin: Peripheral Substituents on Porphyrin Ligand Significantly Affect Film Structure and Charge Mobility, Chemistry – An Asian Journal, 3 (2008) 1092-1103.
[106] M.H. Hoang, Y. Kim, M. Kim, K.H. Kim, T.W. Lee, D.N. Nguyen, S.-J. Kim, K. Lee, S.J. Lee, D.H. Choi, Unusually High-Performing Organic Field-Effect Transistors Based on π-Extended Semiconducting Porphyrins, Advanced Materials, 24 (2012) 5363-5367.
[107] M.H. Hoang, Y. Kim, S.-J. Kim, D.H. Choi, S.J. Lee, High-Performance Single-Crystal-Based Organic Field-Effect Transistors from π-Extended Porphyrin Derivatives, Chemistry – A European Journal, 17 (2011) 7772-7776.
[108] J. Israelachvili, R. Pashley, The hydrophobic interaction is long range decaying exponentially with distance, Nature, 300 (1982) 341-342.
[109] J.N. Israelachvili, Intermolecular and Surface Forces, Academic Press, New York, 1995.
[110] J. Israelachvili, H. Wennerstrom, Role of hydration and water structure in biological and colloidal interactions, Nature, 379 (1996) 219-225.
[111] P. Ball, Water as an Active Constituent in Cell Biology, Chem. Rev., 108 (2008) 74-108.
[112] L. Verma, P.G. Vekilov, J.C. Palmer, Solvent Structure and Dynamics near the Surfaces of β-Hematin Crystals, The Journal of Physical Chemistry B, 125 (2021) 11264-11274.
[113] R.G. Chakrabarti, P.G. Vekilov, Attraction between Permanent Dipoles and London Dispersion Forces Dominate the Thermodynamics of Organic Crystallization, Crystal Growth & Design, 20 (2020) 7429-7438.